Lab on a Chip

CRITICAL REVIEW

Light-assisted direct-write of 3D functional biomaterials

Kolin C. Hribar, Pranav Soman, John Warner, Peter Chung and Shaochen Chen*

Light-assisted 3D direct-printing of biomaterials and cellular-scaffolds has the potential to develop novel lab-on-a-chip devices (LOCs) for a variety of biomedical applications, from drug discovery and diagnostic testing to *in vitro* tissue engineering and regeneration. Direct-writing describes a broad family of fabrication methods that typically employ computer-controlled translational stages to manufacture structures at multi-length scales. This review focuses on light-assisted direct-write fabrication for generating 3D functional scaffolds with precise micro- and nano-architecture, using both synthetic as well as naturally derived biomaterials. Two bioprinting approaches are discussed in detail – projection printing and laser-based systems – where each method is capable of modulating multiple scaffold parameters, such as 3D architecture, mechanical properties (*e.g.* stiffness), Poisson's ratio, chemical gradients, biological cell distributions, and porosity. The light-assisted direct-writing techniques described in this review provide the reader with alternative approaches to fabricate 3D biomaterials for utility in LOCs.
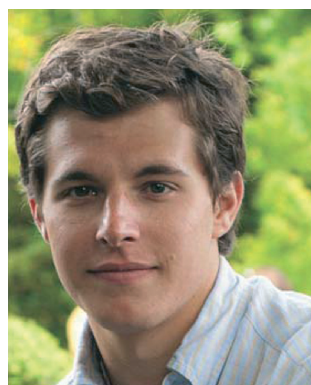
I. Introduction

Over the years, lab-on-a-chip platforms (LOCs) have been extensively developed for the measurement of fundamental biological components (blood glucose, coagulation, cardiac), health biomarkers (metabolic disorders), and infectious agents (pathogens, viruses, anthrax), and have been used for *in vitro* diffusion models (*e.g.* protein kinetic measurements, glucose concentration monitoring) as well as human tissue models (heart, lung, liver on a chip).[1,2] More recently, researchers have sought to develop LOCs with 3D multicellular environments

Department of NanoEngineering, University of California, San Diego, 9500 Gilman Drive, La Jolla, CA 92093, USA. E-mail: chen168@eng.ucsd.edu

better mimicking native tissue while permitting user controlled modification.[2,3] Bioprinting platforms for these types of tissue engineered constructs have immense potential in generating more physiologically relevant LOCs, enabling the rapid screening of toxins, drugs, and ligands in addition to investigating fundamental cell biology in a more native, yet controllable micro/nano 3D environment.[4,5]

The evolving fields of tissue engineering and regeneration, and in larger context, bioengineering and its associated areas, have advanced in tissue culture in order to mimic one or several aspects of the physiological/pathophysiological environment.[6–9] This refinement has progressed from two-dimensional (2D) extracellular matrix (ECM)-coated substrates to three-dimensional (3D) patterned scaffolds for cell

Kolin C. Hribar is a PhD student at UC San Diego in the Department of Nanoengineering working under Dr. Shaochen Chen. He received his B.S. (2010) and M.S. (2011) in Bioengineering from the University of Pennsylvania. His work focuses on generating 3D scaffolds for tissue engineering applications using various biofabrication methods.

Kolin C. Hribar

Pranav Soman is an assistant professor at Syracuse University (SU) in the Departments of Biomedical and Chemical Engineering. He directs the laboratory for Additive Biomaterials Manufacturing at SU, which is broadly interested in developing 3D bioprinting platforms with applications in biomedical engineering.

Pranav Soman

seeding and encapsulation. 2D refers to flat substrates with cell–substrate interactions primarily in the *XY* plane and negligible interactions along the *z*-direction. 3D substrates consist of either defined or random anisotropic architecture along the *z*-direction. Several studies have demonstrated that cells grown in 2D cultures display inconsistencies with the physiological *in vivo* environment with respect to morphology, cell–cell and cell–ECM contacts, proliferation and differentiation.[10] Thus, research has prompted the development of various biofabrication methods in order to more effectively recreate the native 3D tissue.[11]

3D biofabrication is primarily divided into two types: computer-assisted and process-directed techniques. Process-driven fabrication methods – those which do not utilize computer control or direct placement – include freeze-drying,[12] salt leaching,[13] electrospinning,[14] porogen melting[15] gas foaming,[16] and fiber deposition.[17] These methods allow control over bulk physical properties (*e.g.* material stiffness, swelling, *etc.*), however the resulting internal architecture is relatively uncontrolled. Computer-assisted direct-writing approaches, on the other hand, are capable of precisely dictating the internal architecture at the micro- and nanoscale, and thus facilitating greater control at the cellular and subcellular level.

Direct-writing techniques, typically referred to as free-form fabrication or rapid prototyping, are well suited to manufacture 3D scaffolds with orthogonal control over fabrication parameters.[18,19] In most cases, a user-defined 3D structure is modeled using a computer software and broken down into a series of transverse-plane image slices. These slices are created as thin 2D layers for stacking in a layer-by-layer fashion (additive manufacturing), and a 3D scaffold is fabricated according to these image slices by translating either the computer-controlled

Shaochen Chen

Shaochen Chen is a Professor in the Nanoengineering Department at the University of California, San Diego (UCSD). He is also a faculty member of the Institute of Engineering in Medicine and Clinical and Translational Research Institute at UC San Diego. Before joining UCSD, Dr. Chen had been a Professor and a Pearlie D. Henderson Centennial Endowed Faculty Fellow in Engineering at the University of Texas at Austin. From 2008 to 2010, Dr. Chen served as the Program Director for the Nanomanufacturing Program in the National Science Foundation (NSF). Dr. Chen's primary research interests include: Biomaterials and Bioprinting, Tissue Engineering and Regenerative Medicine, Laser Nanomanufacturing, Nanophotonics and Biophotonics. Among his numerous awards, Dr. Chen received the CAREER award from NSF in 2001 and the Young Investigator award from the Office of Naval Research (ONR) in 2004.

stage or the deposition source in *XYZ* directions. Direct-writing allows the investigation of one or several biophysical parameters such as internal-architecture and mechanical properties. This approach also permits the use of a wide array of physiological components, such as biochemicals and encapsulated cells, in a modular fashion. Within the confines of direct-writing, the utility of light (*e.g.* laser or UV) offers a precise, rapid, and cost-effective way to fabricate 3D bio-structures at the micro- and nanoscale. This review will discuss two light-assisted direct-write bioprinting platforms and applications of each: (A) projection printing and (B) laser-based systems, in addition to highlighting some commonly used biomaterials.

Biomaterials

Numerous monomers and a selection of photoinitiators provide many permutations of materials for light-assisted fabrication systems.[19] Monomers of different chain lengths and chemical species at varying concentrations can be used to tune mechanical properties, porosity, and osmotic swelling of the resulting polymerized gels. Modulation of light intensity can also vary the degree of polymerization, additionally affecting these parameters. Though many conventional hydrogels such as agarose and polyacrylamide have been used in light-assisted printing, we will focus on three extensively-utilized, biocompatible, photocurable biomaterials which form hydrogels through free-radical photopolymerization: synthetic poly(ethylene glycol) diacrylate (PEGDA),[20,21] and naturally-derived gelatin methacrylate (GelMA)[22] and hyaluronic acid (HA).[23] For a more complete list of polymers used in hydrogel fabrication, the reader is asked to consult the ref. 24 and 25.

PEGDA provides an excellent material for biomedical applications because of its high water content, biocompatibility and tunable mechanical properties.[26] Like many monomers, PEGDA may be synthesized at different molecular weights (typically 700–10 000 Da, in accordance to the number of polymer chains) and poly-distributions to generate polymerized gels of varying crosslinking densities and materials properties (*e.g.* stiffness, swelling, porosity). Moreover, multiple PEGDA monomers may be mixed at different concentrations to further alter the aforementioned material properties (*e.g.* 10 kDa PEGDA mixed with 700 Da PEGDA). Some synthetic materials like PEGDA are nondegradable, however chemical modification or mixing with other materials (*e.g.* DTT) may achieve a predictable degradation effect.[27] For cell seeding, PEG scaffolds require the grafting of adhesive peptide sequences (*e.g.* RGDS and YIGSR) or adhesive proteins (*e.g.* fibronectin and laminin).

Naturally derived hydrogels made from gelatin methacrylate (GelMA) have biologically active sequences that bind key integrins, enabling cells to adhere and migrate onto the structure.[22,28] GelMA is generally a xenogenic modified macromer, therefore relatively inexpensive depending on the source and has the associated limitations *in vivo*. Hyaluronic acid (HA), a naturally occurring native ECM component and FDA-approved

biomaterial, is a non-immunogenic polymer known to be important in wound healing. For instance, exogenous HA has been shown to reduce scar formation and promote regeneration in peripheral nerve injuries.[23] Since various biochemical moieties can be functionally introduced along the HA polymer backbone, a photopolymerizable form of HA has been created through the addition of methacrylate groups, termed glycidyl methacrylate-modified HA (GMHA). GMHA scaffold surfaces can be further modified to incorporate the cell-adhesive protein laminin. The library of photopolymerizable materials continues to expand with the development and modification of new and existing monomers/macromers, respectively, such as the aforementioned GMHA and GelMA, and thus light-assisted printing has the ability to work with an abundance of materials.

II. Projection printing systems

Digital mask (*i.e.* "maskless") projection printing is a type of stereolithography which uses a digital micro-mirror device (DMD) found in conventional computer projectors to polymerize and solidify a photosensitive liquid prepolymer using either UV or other light sources.[19,21,29–36] Fig. 1A shows a version of the maskless projection printing system called the dynamic optical projection stereolithography (DOPsL) platform.[20,21,37–42] The "maskless" or digital mask option allows for the use of controllable and interchangeable reflected light patterns rather than static, more expensive physical masks (such as those used in photolithography). The system spatially modulates collimated UV light using a DMD chip (1920 × 1080 resolution) to project custom-defined optical patterns onto a photocurable prepolymer solution. The DMD chip serves as an array of reflective coated aluminum micro-mirrors, capable of redirecting light to two states [0,1], tilted with two bias electrodes to form angles of either +12° or −12° with respect to the surface. Illumination from the light source reflects into the projection lens only when the micro-mirror is in its arbitrary "on" state. In the "off" state, the pixel appears dark as the illuminated light is reflected away from the projection lens.

To generate 3D structures, projection stereolithography platforms such as DOPsL employ a layer-by-layer fabrication procedure. Often, a 3D computer rendering (made with a CAD software or CT scans) is deconstructed into a series of evenly spaced planes, or layers. The pattern for each layer is
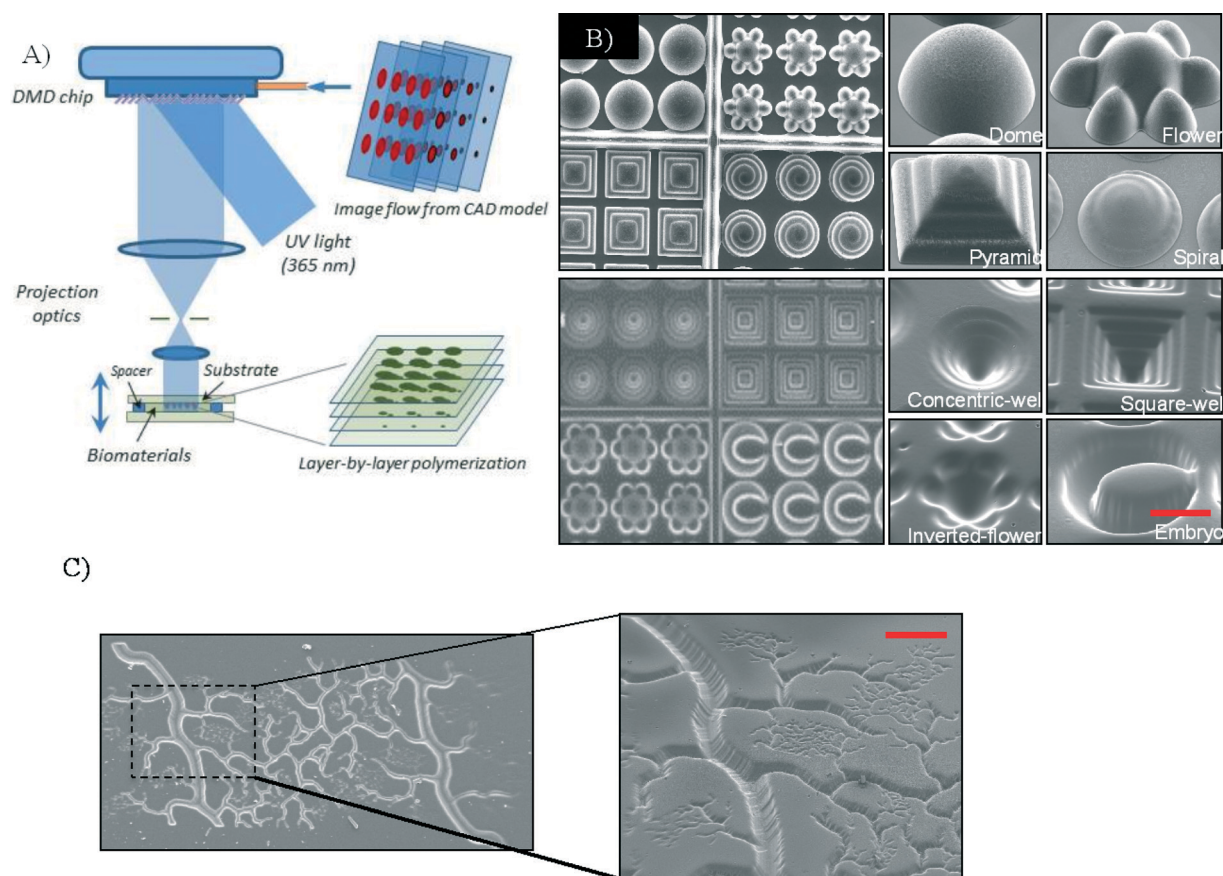
Fig. 1 (A) Schematic of a projection printing setup called dynamic optical projection stereolithography (DOPsL): UV-light illuminates the DMD mirror system, which generates an optical pattern according to the image flow from the control computer. The optical pattern is projected through an optical lens and onto the photosensitive biomaterial to fabricate a 3D scaffold in a layer-by-layer manner. (B) SEM images of the concave and convex features (*e.g.* domes, microwells, *etc.*) using PEGDA demonstrating the versatility of the biofabrication system.[41] (C) SEM image of a complex vasculature in PEGDA fabricated from a CAD file. Scale bar = 100 μm.

displayed on the DMD chip, exposing UV light onto the photocurable material. After one layer is patterned, the substrate is lowered using an automated stage and the next pattern is displayed. The user has control over the stage speed, intensity of the light, and height of the structure, allowing for the fabrication of various complex structures, such as spiral domes, pyramids and microwells (Fig. 1B).[41] Fig. 1C demonstrates a complex vascular structure fabricated in PEGDA using this technology, another example of its versatility. As previously mentioned, mimicking the native tissue microenvironment with respect to architecture and material properties is key to the design of these 3D biostructures.

We will illustrate projection printing's increasing importance and utility in the tissue engineering field with several examples. From Gauvin et al., hydrogels comprised of GelMA were fabricated in 3D log-pile and hexagonal layered constructs (Fig. 2A).[22] Mechanical properties were varied by the geometry and prepolymer concentration (Fig. 2B), and following, cell migration and proliferation into the scaffolds were monitored (Fig. 2C). Log-pile and hexagonal structures displayed different moduli even when the prepolymer solution remained constant (10% GelMA). Importantly, the results from this study demonstrated the capability of the projection printing systems to generate cell-compatible scaffolds with tailored mechanical properties (by either varying prepolymer concentration or the micro-architecture). In another example, Lin et al. utilized projection printing to investigate cellular responses to varying scaffold porosities (Fig. 3A).[34] After encapsulating adipose-derived stem cells within the structures and incubating for seven days, an MTS assay reported a higher cell viability and activity of the cells in porous structures than in solid, non-porous structures (Fig. 3B).

Another parameter in tissue engineering – Poisson's ratio (PR) – has also been investigated using projection printing.[39,40,42] In general, the mechanical properties of a biomaterial scaffold can be quantitatively described by its elastic modulus and PR. Elastic modulus of the underlying substrate describes the material's elastic behavior during loading, while PR refers to the degree at which the scaffold contracts/expands in the transverse direction. Previously, research has extensively reported on the connection between a substrate's elastic modulus and cell response.[43,44] PR has been less explored with conventional manufacturing approaches (e.g. annealing of polyurethane foams), because they offer little control over the microarchitecture.[45,46] Light-assisted direct-writing, on the other hand, can provide precise control over this parameter. For instance, our lab used the DOPsL platform to fabricate unit-cell geometries for negative Poissson's ratio (NPR) (re-entrant structure, missing rib model) and zero Poisson ratio (ZPR) (semi-reentrant structure) scaffolds (Fig. 4A). Fig. 4B shows a structure undergoing tensile stress and expanding in the transverse direction, thereby demonstrating NPR. Analysis of the PR effect according to several unit-cells is documented in Fig. 4C. Scaffolds exhibiting NPR (those which expand upon application of tensile stress) or ZPR may be more suitable for emulating the behavior of certain native
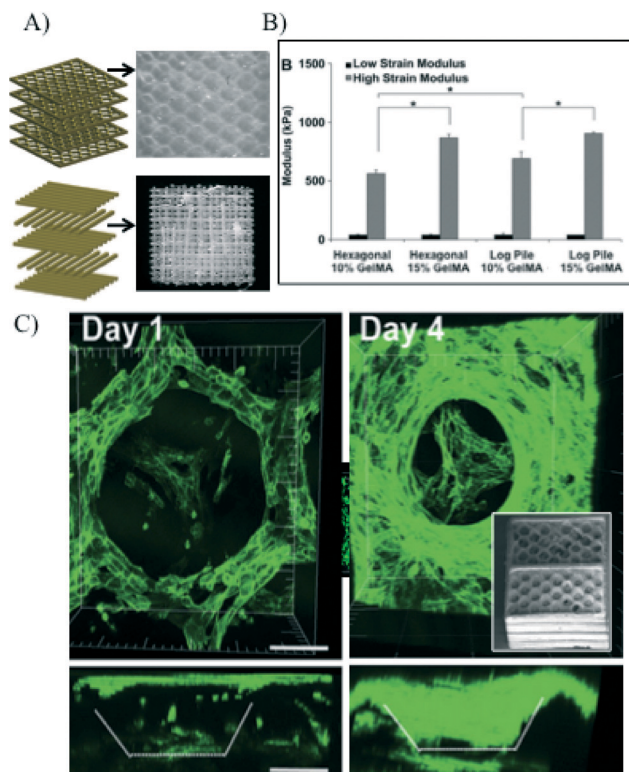

Fig. 2 (A) Schematic shows layer-by-layer manufacturing of log-pile and hexagonal internal architecture. Optical images depict 3D scaffolds using GelMA biomaterial. (B) Mechanical properties of scaffolds having hexagonal or log-pile structures using various GelMA percentages. Prepolymer concentration and engineered structures can be used to tailor the mechanical properties of the GelMA scaffolds. * indicates statistical significance ($p < 0.05$). (C) 3D confocal images showing scaffold coverage by the HUVEC-GFP cells and cell penetration into the porous structure as a function of time; inset: SEM image of hexagonal layered scaffold.[22] Scale = 100 μm.

tissues (e.g. expansion in blood vessels), and could be further investigated with projection printing.

These examples and others serve to demonstrate the versatility of projection printing systems in fabricating complex 3D structures of varying topographical features, mechanical properties, and porosity. Additionally, projection printing offers superior fabrication speeds (e.g. DOPsL fabricates within seconds) as compared to serial writing of two/multiple-photon polymerization.[19,41] However, limitations include the resolution feature size (due to limitations of the projection lens and material swelling), the requirement of using photopolymerizable materials, and the effect of UV exposure to cells and photosensitive biomaterials.[19,47] Improved optics will continue to enhance the resolution, and the expanding library of photopolymerizable materials will allow for increased scaffold complexity.

III. Laser-based techniques

Many of the concepts introduced with the projection-based systems, including material selection, geometry optimization, cell seeding and encapsulation design, also apply to the
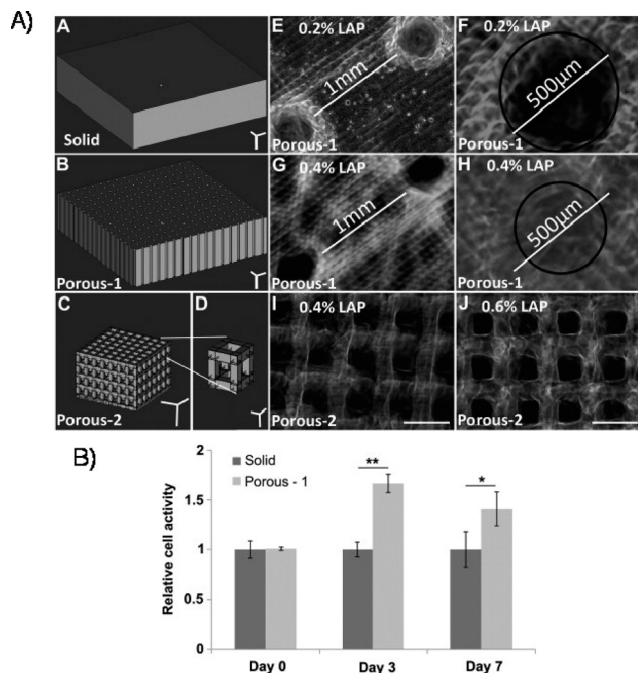
Fig. 3 (A) 3D gels of varying porosity fabricated by projection stereolithography, with the CAD drawings and resulting internal architectures. Scale bar = 500 μm unless otherwise indicated. (B) Relative cell activity assessed by MTS assay, using either solid or porous scaffolds.[34]

laser-based systems.[18] Historically, laser-based printing techniques such as laser-direct-writing,[48,49] laser-induced forward

transfer (LIFT),[50] matrix-assisted pulsed laser evaporation (MAPLE)[51] *etc.*, have been used to spatially pattern cells in 2D,[52,53] with limitations of low cell viability and throughput. Recently, 3D laser bioprinting has evolved to additive manufacturing (*e.g.* layer-by-layer).[54–56]

3D laser direct-writing incorporates a CAD model numerically sliced into a series of 2D layers, and fabricates 3D structures utilizing a motorized stage (controlled in *XYZ*) to manipulate the sample or laser (Fig. 5A).[33,57] Laser-based fabrication differs from projection printing primarily in its light source,[58–60] where a laser focused through an objective lens is used to crosslink and polymerize a liquid biopolymer. Writing width can be modulated and controlled by exposure energy – dictated by the beam size and laser power – and writing speed. After the first layer is crosslinked, the stage moves downward and a new layer of polymer is solidified according to the design. One such system, termed SLA (stereolithography apparatus), employs a focused single-photon UV laser to polymerize photocurable materials.[57] Chan *et al.* used SLA for generating controlled 3D structures to co-culture a heterogeneous cell distribution and assess long-term cell viability (Fig. 5B). In a similar laser setup, Mapili *et al.* demonstrated a multilayer PEG hydrogel scaffold functionalized with heparin or RGD-peptide sequences for cell adhesion (Fig. 5C).[61]

Two-photon polymerization (TPP) is another type of laser-based direct-writing which uses focused near-infrared (NIR) femtosecond laser pulses (wavelength ~800 nm) to trigger
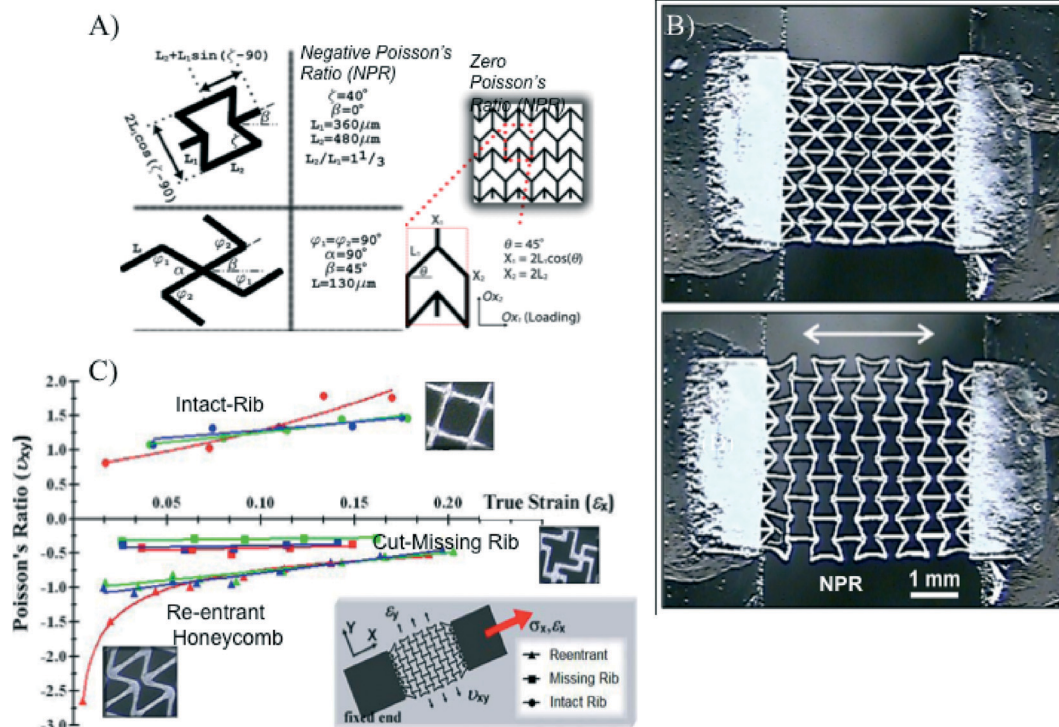

Fig. 4 (A) Unit-cell parameters and relevant dimensional parameters of NPR (reentrant honeycomb, cut missing rib) and ZPR (semi-re-entrant) architectures. The walls of the unit-cells (denoted as ribs) are approximately 40 μm wide and 50–100 μm deep. (B) PEGDA scaffolds with NPR expand with application of strain in the *X*-axis (white arrow). Scale = 1 mm. (C) Measured Poisson's ratio as a function of true strain for single-layer PEGDA scaffolds composed of the reentrant, missing-rib, and intact-rib (control) unit-cell geometries.[42]
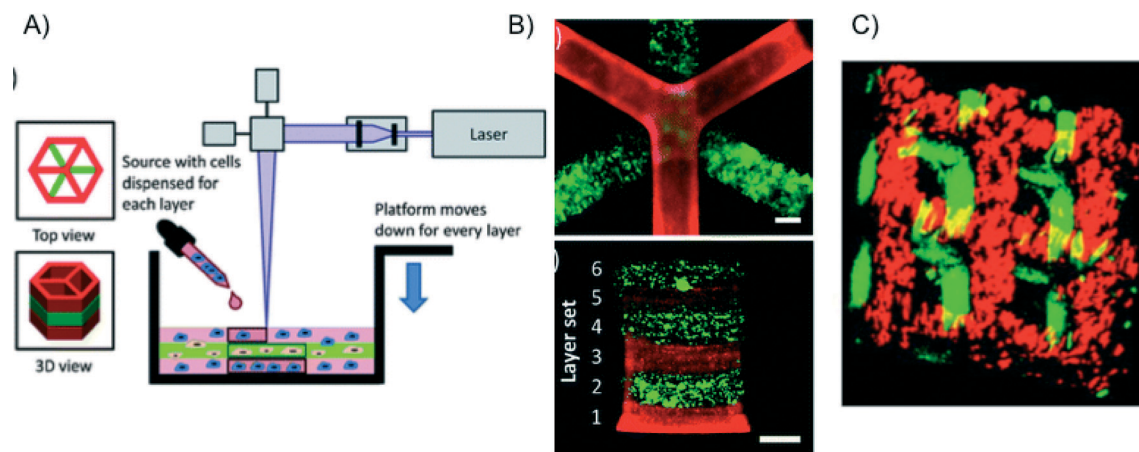
Fig. 5 (A) Schematic of laser stereolithography using SLA (stereolithography apparatus).[57] (B) Resulting SLA-fabricated 3D hydrogels with six layers.[57] Scale bars = 1 mm. (C) Spatially-patterned 3D scaffolds fabricated by laser-assisted stereolithography.[61]
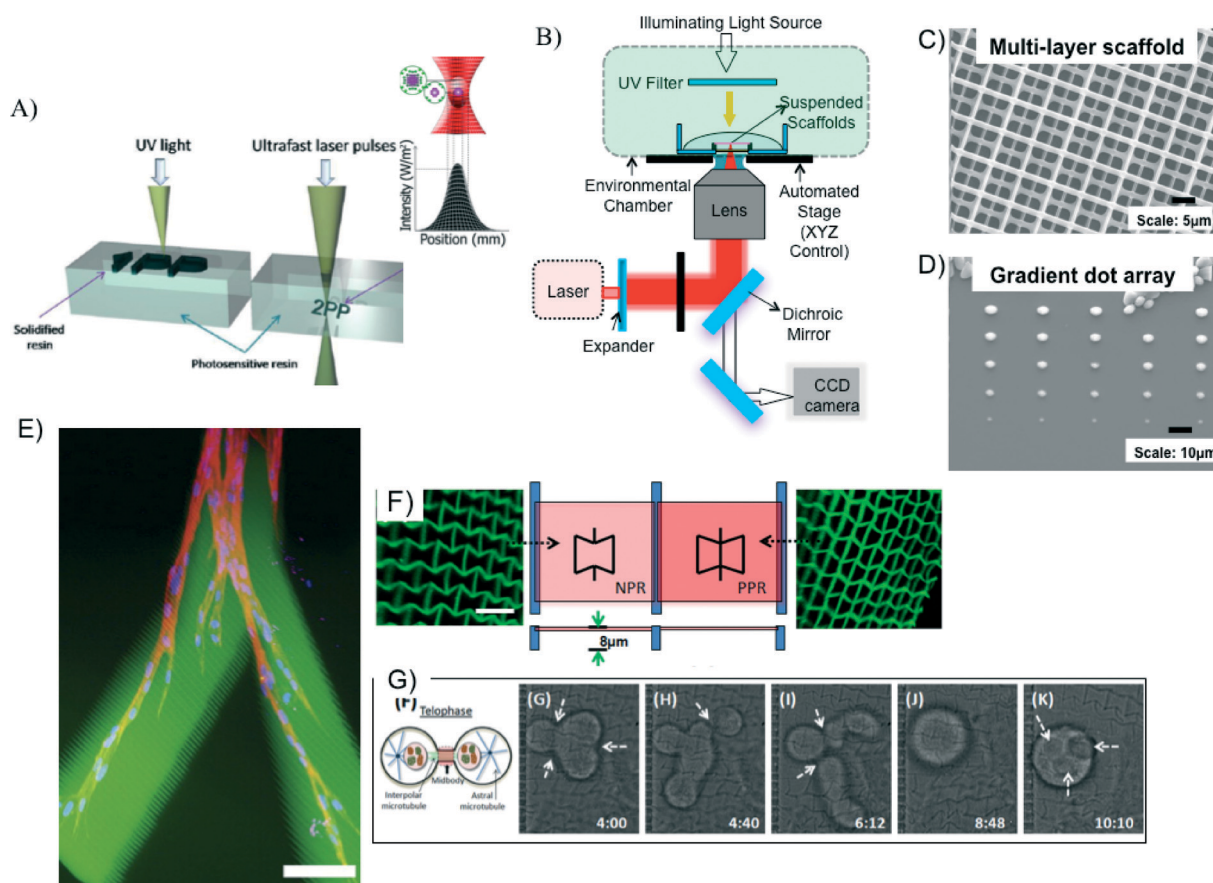

Fig. 6 (A) Principle of operation for single- and two-photon polymerization.[69] (B) Schematic of femtosecond laser fabrication set-up. (C) Multi-layer log-pile scaffold with ~1 μm features.[66] (D) Gradient dot array at sub-micron resolution (the largest dot size ~4 μm, with spacing ~20 μm) fabricated by decreasing the laser-power from top to bottom. Biochemicals such as growth factors can be incorporated in these arrays.[66] (E) 3D migration of cells within an RGD-modified PEG hydrogel, fabricated by TPP. Scale bar = 100 μm.[67] (F) NPR and PPR structures patterned with TPP, and (G) time-resolved single cell studies on an NPR structure (for details on this study, please refer to ref. 68).

crosslinking of a photosensitive biomaterial.[62] In this fabrication technique, simultaneous absorption of two NIR photons generates free radicals to initiate the polymerization of volume-blocks (voxels).[63–65] A distinct advantage of this system is the nonlinear nature of the laser–material interaction, achieving feature sizes below the diffraction limit of applied light. This process allows for better resolution at the expense of slower speeds and limited scalability (due to

restrictions of the objective lens' working distance) compared to single photon polymerization (*e.g.* SLA) (Fig. 6A). Fig. 6B shows a typical TPP laser setup. In tissue engineering applications, TPP has been exploited to generate precise micro-scale biomaterial structures. For instance, in Fig. 6C, TPP was used to fabricate a 3D log-pile structure (1 micron width lines) made of PEGDA with spacing of 8 μm. In another example, a gradient array of microdots (2–10 microns in diameter) was fabricated using a mixture of PEGDA and Cultrex 3-D Culture Matrix, a type of standardized basement membrane extract (Fig. 6D).[66] Lee *et al.* also demonstrated TPP fabrication of RGD-modified hydrogels to dictate cell migration in 3D (Fig. 6E).[67] These examples demonstrate TPP's ability to chemically pattern and generate biostructures at cellular and subcellular scales.

Additionally, one can use TPP to explore the interaction of topographical features and single cell response. Similar to a study described in the projection printing section, Zhang *et al.* fabricated PEGDA-derived scaffolds exhibiting either NPR or PPR (negative or positive Poisson's ratio, respectively) (Fig. 6F).[68] Cell motility, orientation, and proliferation varied between NPR and PPR constructs, suggesting that PR plays a role in cell fate (Fig. 6G); further tests are needed to promote this claim, however. Importantly, single cell studies are possible with TPP due to its high resolution of fabrication, compared to single photon or projection printing.

Conclusion

Both projection printing (*e.g.* DOPsL) and laser-based direct-writing systems (SLA, TPP) offer promising technologies to fabricate 3D bioconstructs with precise micro- and nano-architecture. Though these processes require photopolymerizable materials, the library of such materials continues to expand, accommodating for various scaffold properties (*e.g.* stiffness, porosity, swelling) in a 3D setting. Additionally, projection printing allows for the rapid printing of various complex structures, demonstrating its potential for high throughput screening. Though typically slower than projection printing (and SLA), TPP provides a high-resolution alternative to direct-writing for the fabrication of nanoscale features, and could play a significant role in single cell analysis in the years to come. More interesting yet, combining several platforms such as projection printing and TPP could enable researchers to study a multitude of parameters in 3D. Light-assisted direct-writing could also complement non-light-assisted direct-writing platforms (*e.g.* nozzle-based or extrusion systems) for generating precise nano/microscale features and chemical patterning within a larger scaffold. In the years ahead, we welcome the convergence of multiple printing technologies in the pursuit of growing physiologically relevant 3D tissue constructs *in vitro* (*i.e.* tissue-on-a-chip). Such *in vitro* biomimetic LOCs will enable us to more accurately answer basic cell biology questions and monitor various testing parameters (*e.g.* drug toxicity/discovery, (patho)physiology) prior to more expensive *in vivo* models.

References

1 C. D. Chin, V. Linder and S. K. Sia, *Lab Chip*, 2012, **12**, 2118–2134.

2 A. M. Ghaemmaghami, M. J. Hancock, H. Harrington, H. Kaji and A. Khademhosseini, *Drug Discovery Today*, 2012, **17**, 173–181.

3 D. E. Ingber and G. M. Whitesides, *Lab Chip*, 2012, **12**, 2089–2090.

4 M. Baker, *Nature*, 2011, **471**, 661–665.

5 D. Huh, Y.-S. Torisawa, G. A. Hamilton, H. J. Kim and D. E. Ingber, *Lab Chip*, 2012, **12**, 2156–2164.

6 I. R.-D. Jorge, Z. Bimeng, R. Daniel, S. Zhi-dong and X. Tao, *Biofabrication*, 2012, **4**, 035001.

7 P. X. Ma, *Adv. Drug Delivery Rev.*, 2008, **60**, 184–198.

8 R. Langer and J. P. Vacanti, *Science*, 1993, **260**, 920–926.

9 L. G. Griffith and G. Naughton, *Science*, 2002, **295**, 1009–1014.

10 A. J. Engler, M. A. Griffin, S. Sen, C. G. Bönnemann, H. L. Sweeney and D. E. Discher, *J. Cell Biol.*, 2004, **166**, 877–887.

11 F. Pampaloni, E. G. Reynaud and E. H. K. Stelzer, *Nat. Rev. Mol. Cell Biol.*, 2007, **8**, 839–845.

12 F. J. O'Brien, B. A. Harley, I. V. Yannas and L. Gibson, *Biomaterials*, 2004, **25**, 1077–1086.

13 S. B. Lee, Y. H. Kim, M. S. Chong, S. H. Hong and Y. M. Lee, *Biomaterials*, 2005, **26**, 1961–1968.

14 X. Zong, H. Bien, C.-Y. Chung, L. Yin, D. Fang, B. S. Hsiao, B. Chu and E. Entcheva, *Biomaterials*, 2005, **26**, 5330–5338.

15 A. S. P. Lin, T. H. Barrows, S. H. Cartmell and R. E. Guldberg, *Biomaterials*, 2003, **24**, 481–489.

16 R. Nazarov, H.-J. Jin and D. L. Kaplan, *Biomacromolecules*, 2004, **5**, 718–726.

17 L. Moroni, J. R. de Wijn and C. A. van Blitterswijk, *Biomaterials*, 2006, **27**, 974–985.

18 I. Antoniac, T. Billiet, M. Vandenhaute, J. Schelfhout, S. Vlierberghe and P. Dubruel, in *Biologically Responsive Biomaterials for Tissue Engineering*, Springer, New York, 2013, pp. 201–249.

19 T. Billiet, M. Vandenhaute, J. Schelfhout, S. Van Vlierberghe and P. Dubruel, *Biomaterials*, 2012, **33**, 6020–6041.

20 L. H. Han, G. Mapili, S. Chen and K. Roy, *J. Manuf. Sci. E–T. ASME*, 2008, **130**, 021005.

21 Y. Lu, G. Mapili, G. Suhali, S. C. Chen and K. Roy, *J. Biomed. Mater. Res., Part A*, 2006, **77**, 396–405.

22 R. Gauvin, Y.-C. Chen, J. W. Lee, P. Soman, P. Zorlutuna, J. Nichol, S. C. Chen and A. Khademhosseini, *Biomaterials*, 2012, **33**, 3824–3834.

23 S. Suri, L. H. Han, W. Zhang, A. Singh, S. C. Chen and C. E. Schmidt, *Biomed. Microdevices*, 2011, **13**, 983–993.

24 K. T. Nguyen and J. L. West, *Biomaterials*, 2002, **23**, 4307–4314.

25 J. L. Ifkovits and J. A. Burdick, *Tissue Eng.*, 2007, **13**, 2369–2385.

26 B. Baroli, *J. Pharm. Sci.*, 2007, **96**, 2197–2223.

27 G. A. Hudalla, T. S. Eng and W. L. Murphy, *Biomacromolecules*, 2008, **9**, 842–849.

28 A. I. Van Den Bulcke, B. Bogdanov, N. De Rooze, E. H. Schacht, M. Cornelissen and H. Berghmans, *Biomacromolecules*, 2000, **1**, 31–38.

29 J.-W. Choi, R. Wicker, S.-H. Lee, K.-H. Choi, C.-S. Ha and I. Chung, *J. Mater. Process. Technol.*, 2009, **209**, 5494–5503.

30 A. D. Lantada, P. L. Morgado and J. Stampfl, in *Handbook on Advanced Design and Manufacturing Technologies for Biomedical Devices*, Springer, US, 2013, pp. 181–205.

31 T. J. Horn and O. L. A. Harrysson, *Sci. Prog.*, 2012, **95**, 255–282.

32 S. D. Gittard and R. J. Narayan, *Expert Rev. Med. Devices*, 2010, **7**, 343–356.

33 A. Waldbaur, H. Rapp, K. Lange and B. E. Rapp, *Anal. Methods*, 2011, **3**, 2681–2716.

34 H. Lin, D. Zhang, P. G. Alexander, G. Yang, J. Tan, A. W. Cheng and R. S. Tuan, *Biomaterials*, 2013, **34**, 331–339.

35 R. Liska, M. Schuster, R. Inführ, C. Turecek, C. Fritscher, B. Seidl, V. Schmidt, L. Kuna, A. Haase, F. Varga, H. Lichtenegger and J. Stampfl, *J. Coat. Technol. Res.*, 2007, **4**, 505–510.

36 L. H. Han, G. Mapili, S. Chen and K. Roy, *J. Manuf. Sci. E–T. ASME*, 2008, **130**, 021005.

37 P. Soman, J. A. Kelber, J. W. Lee, T. N. Wright, K. S. Vecchio, R. L. Klemke and S. Chen, *Biomaterials*, 2012, **33**, 7064–7070.

38 P. Soman, B. T. D. Tobe, J. W. Lee, A. Winquist, I. Singec, K. S. Vecchio, E. Y. Snyder and S. Chen, *Biomed. Microdevices*, 2012, **14**, 829–838.

39 P. Soman, D. Y. Fozdar, J. W. Lee, A. Phadke, S. Varghese and S. Chen, *Soft Matter*, 2012, **8**, 4946–4951.

40 P. Soman, J. W. Lee, A. Phadke, S. Varghese and S. Chen, *Acta Biomater.*, 2012, **8**, 2587–2594.

41 A. P. Zhang, X. Qu, P. Soman, K. C. Hribar, J. W. Lee, S. Chen and S. He, *Adv. Mater.*, 2012, **24**, 4266–4270.

42 D. Y. Fozdar, P. Soman, J. W. Lee, L. H. Han and S. Chen, *Adv. Funct. Mater.*, 2011, **21**, 2712–2720.

43 D. E. Discher, P. Janmey and Y.-L. Wang, *Science*, 2005, **310**, 1139–1143.

44 A. J. Engler, S. Sen, H. L. Sweeney and D. E. Discher, *Cell*, 2006, **126**, 677–689.

45 R. H. Baughman, S. Stafstrom, C. Cui and S. O. Dantas, *Science*, 1998, **279**, 1522–1524.

46 R. Lakes, *Science*, 1987, **235**, 1038–1040.

47 A. Khademhosseini and R. Langer, *Biomaterials*, 2007, **28**, 5087–5092.

48 D. J. Odde and M. J. Renn, *Biotechnol. Bioeng.*, 2000, **67**, 312–318.

49 L. Koch, M. Gruene, C. Unger and B. Chichkov, *Curr. Pharm. Biotechnol.*, 2013, **14**, 91–97.

50 R. S. Nathan, T. C. David, H. Yong, R. Nurazhani Abdul, X. Yubing and B. C. Douglas, *Biofabrication*, 2010, **2**, 032001.

51 P. K. Wu, B. R. Ringeisen, J. Callahan, M. Brooks, D. M. Bubb, H. D. Wu, A. Piqué, B. Spargo, R. A. McGill and D. B. Chrisey, *Thin Solid Films*, 2001, **398–399**, 607–614.

52 A. Doraiswamy, R. J. Narayan, M. L. Harris, S. B. Qadri, R. Modi and D. B. Chrisey, *J. Biomed. Mater. Res., Part A*, 2007, **80**, 635–643.

53 M. O. Christina, W. Xingjia, J. A. Juanita and R. R. Bradley, *Biomed. Mater.*, 2008, **3**, 034101.

54 M. Gruene, M. Pflaum, C. Hess, S. Diamantouros, S. Schlie, A. Deiwick, L. Koch, M. Wilhelmi, S. Jockenhoevel, A. Haverich and B. Chichkov, *Tissue Eng., Part C*, 2011, **17**, 973–982.

55 L. Koch, A. Deiwick, S. Schlie, S. Michael, M. Gruene, V. Coger, D. Zychlinski, A. Schambach, K. Reimers, P. M. Vogt and B. Chichkov, *Biotechnol. Bioeng.*, 2012, **109**, 1855–1863.

56 R. K. Pirlo, P. Wu, J. Liu and B. Ringeisen, *Biotechnol. Bioeng.*, 2012, **109**, 262–273.

57 V. Chan, P. Zorlutuna, J. H. Jeong, H. Kong and R. Bashir, *Lab Chip*, 2010, **10**, 2062–2070.

58 F. P. W. Melchels, J. Feijen and D. W. Grijpma, *Biomaterials*, 2010, **31**, 6121–6130.

59 D. W. Hutmacher, M. Sittinger and M. V. Risbud, *Trends Biotechnol.*, 2004, **22**, 354–362.

60 A. Ovsianikov, M. Gruene, M. Pflaum, L. Koch, F. Maiorana, M. Wilhelmi, A. Haverich and B. Chichkov, *Biofabrication*, 2010, **2**, 014104.

61 G. Mapili, Y. Lu, S. C. Chen and K. Roy, *J. Biomed. Mater. Res., Part B*, 2005, **75**, 414–424.

62 M. Gebinoga, J. Katzmann, U. Fernekorn, J. Hampl, F. Weise, M. Klett, A. Läffert, T. A. Klar and A. Schober, *Eng. Life Sci.*, 2013, **13**, 368–375.

63 R. Landers, A. Pfister, U. Hubner, H. John, R. Schmelzeisen and R. Mulhaupt, *J. Mater. Sci.*, 2002, **37**, 3107–3116.

64 A. Ovsianikov, A. Deiwick, S. Van Vlierberghe, P. Dubruel, L. Moller, G. Dräger and B. Chichkov, *Biomacromolecules*, 2011, **12**, 851–858.

65 E. T. Ritschdorff and J. B. Shear, *Anal. Chem.*, 2010, **82**, 8733–8737.

66 W. Zhang and S. C. Chen, *MRS Bull.*, 2011, 1028–1033.

67 S. H. Lee, J. J. Moon and J. L. West, *Biomaterials*, 2008, **29**, 2962–2968.

68 W. Zhang, P. Soman, K. Meggs, X. Qu and S. Chen, *Adv. Funct. Mater.*, 2013, **23**, 3226–3232.

69 S. Wu, J. Serbin and M. Gu, *J. Photochem. Photobiol., A*, 2006, **181**, 1–11.